Aggregated BESS Dynamic Models for Active Distribution Network Studies

Fabian Calero, *Student Member, IEEE,* Claudio A. Cañizares, *Fellow, IEEE,* and Kankar Bhattacharya, *Fellow, IEEE*

***Abstract*—This paper proposes a transmission-system-level aggregated model of Battery Energy Storage Systems (BESSs) distributed through Active Distribution Networks (ADNs), to study the dynamic performance and services provided by these systems to power grids. ADNs comprise intelligent loads, local generation, particularly solar PV, and BESSs, which can provide different services to transmission grids, including voltage control, oscillation damping, frequency regulation, and active and reactive power injections. Proper equivalent models of the ADN components allow to evaluate the impact and integration of these networks on power grids. In this paper, ADN's measurements of the aggregated response of the BESSs at the boundary bus with the transmission system are used to develop an aggregated black-box model based on two Neural Networks (NNs), one for active power and another for reactive power, with their optimal topology obtained using a Genetic Algorithm (GA). Detailed simulations are performed, using a commercial-grade software for power system analysis, of multiple BESSs connected to a CIGRE benchmark ADN connected to a bus of the 9-bus WSCC benchmark transmission network; the test ADN is then replaced by the proposed black-box model, with aggregated models of the loads and PV generation, demonstrating that the proposed model can accurately reproduce the results obtained.**

***Index Terms*—Aggregated model, Battery Energy Storage System, black-box, distribution systems, neural networks, transmission systems.**

I. Introduction

In recent years, the dropping prices of lithium-ion battery packs, accompanied by the increasing interest of household owners, industry, and commercial customers on installing dependable small-scale renewable generation, particularly solar PV, is boosting the deployment of Battery Energy Storage Systems (BESSs), which facilitate the integration of these Distributed Energy Resources (DERs) at the distribution level, thus transforming distribution grids to Active Distribution Networks (ADNs). These ADNs have the potential of impacting the transmission systems if their operation is coordinated, since ADNs can provide services such as frequency regulation, voltage control, or oscillation damping. However, modeling ADNs in detail for transmission system studies is not practical, since the number of components that need to be modeled in a distribution system is substantial, which not only increases the computational burden of simulations, but also requires knowledge of multiple distribution system parameters, which may not be available to the transmission grid operator. Hence, equivalent aggregated models of ADN loads, generation, and BESSs are being proposed in the literature instead, with Neural Networks (NNs) being widely used to develop black-box models, due their capability to represent highly nonlinear dynamic systems.

Methods to aggregate traditional generating units, electric motors and other types of loads are widely available in the existing literature (e.g., [1]–[4]), whereas aggregated models of power-electronic based generation and energy storage are less common, and still under investigation. Aggregated models of ADNs for transmission system studies have been proposed in [5] and [6], where equivalent gray-box models of ADNs are discussed, based on active and reactive power measurements at the point of connection with the transmission system. These equivalent models comprise a converter-connected generator and a composite load model in parallel, which can successfully reproduce the results of detailed simulations; however, these models do not allow simulating changes in the operating points of the generating units within the ADNs, and, furthermore, BESSs are not considered. In [7], a grey-box model of an ADN is proposed, which includes Inverter Based Generators (IBGs) and BESSs, whose parameters are optimally obtained based on frequency-domain comparisons of the model's simulation predictions and measurements of active and reactive power injections at the transmission-distribution interface. However, only one type of disturbance (short circuit) is used to train the aggregated model; the BESSs and IBGs are presented as a single aggregated element, which neglects the fact that BESS could be operating in charging or discharging mode, or providing other grid services; and the aggregated IBG model considers the dynamics of the VSC's current control only, thus neglecting the dynamics of additional controllers, such as those of voltage or frequency controllers. In [8], the same ADN from [7] is studied representing the BESSs as an independent element; however, the same converter model is used to aggregate the BESSs and the IBGs, hence still limiting the possibility of representing the BESS in the provision of grid services, such as frequency or voltage regulation.

More complex aggregated ADN models have been proposed, for example in [9], where the ADN considers loads, motors and IBGs, with the latter allowing the representation of the dynamics of Phase Locked Loop (PLL), voltage transducers, and other VSC controls required by grid codes, such as Low Voltage Ride-Through (LVRT) capability, reactive power injection, active power recovery, and IBGs partial tripping; these result in an aggregated ADN model with 40 tunable

This work has been supported by Canada's NSERC Energy Storage Technology (NEST) Network (https://nrc.canada.ca/en).

The authors are with the Department of Electrical and Computer Engineering, University of Waterloo, Waterloo, ON, N2L 3G1, Canada (e-mail: fcalero@uwaterloo.ca; ccanizar@uwaterloo.ca; kankar@uwaterloo.ca).

parameters. However, BESSs are not considered as part of the ADN, and the model is developed to represent only a single type of disturbance, i.e., transmission voltage dips. In [10], an aggregated gray-box model of an ADN is presented, which comprises a converter-connected synchronous generator, in parallel with a composite-based load, i.e., an induction motor and zip load model, representing dynamic and static load components, respectively; the equivalent gray-box model of the ADN is thus represented with a seventh-order state-space model, which is linearized around a specific operating point, and whose parameters are obtained by minimizing the error of model output with respect to simulations of a detailed ADN model. The high voltage transmission system is modeled as a single synchronous machine, and the test ADN is based on the Medium Voltage (MV) CIGRE benchmark system; two sets of training data are used to tune the gray-box model, including short circuits and step changes in the load. Even though the model is shown to yield accurate predictions, the results are restricted to the initial operating condition of the ADN, due to the linearization process, and thus it might not accurately represent online simulations of other system conditions that may be found during real-time operation. In [11], a state-space equivalent of a distribution system connected to a transmission grid is studied, whose parameters are obtained based on measurements of active and reactive power, and voltage and frequency at the boundary bus. The disadvantage of these aggregated models is that they are based on traditional generating units, i.e., steam, hydro and diesel. An aggregated gray-box model of ADNs consisting of several Microgrids (MGs) with BESSs for frequency stability studies is proposed in [12]. The model is based on first order transfer functions, the parameters of which are obtained using Prony analysis on measurements of active power at the ADN boundary bus and the upward grid, plus a clustering approach based on similar responses of the MGs in the ADN. However, only inverter-based and synchrnonus generators are considered in the ADN, and multiple transfer functions representing clusters of generators within the gray-box model are required. More simplified models have been proposed, such as the one in [13], where the model of an HVDC link is used to represent the aggregation of disperse BESSs connected in distribution systems, to study the transient stability of a transmission system; however, the authors do not discuss the aggregation process or the effectiveness of the proposed BESS model.

Black-box models based on NNs have also been used to represent equivalent ADNs. For example, in [14], a recurrent-NN black-box model is proposed to represent a distribution system connected to a transmission grid; however, only fuel cells and microturbines are considered as DERs, and the aggregated model is developed based only on voltage disturbances at the boundary bus with the transmission system. In [15], recurrent NNs are proposed to model part of a transmission system. The NN black-box model is connected to the transmission gird at three different points, using measurements of the voltages at each boundary point as inputs, and yielding current phasor injections as outputs; however, the power system modeled is based on rotating machines only.

None of the aforementioned works have examined the aggregation of BESSs, which are different from other DERs in that they can act as both loads and generators. Furthermore, the dynamic response of a BESSs to contingencies can be substantially different from the typical behaviour of a rotating-machine based generator, due to their fast response and ability to operate as loads to enhance the provision of services such as frequency and voltage regulation, oscillation damping, and power injections. In view of the above, the objective of this paper is to propose a NN-based black-box model to reproduce the aggregated response, at the transmission system level, of BESSs distributed within an ADN. Since, as discussed in some of the existing works, aggregated gray-box models, have the limitation of mostly being effective to reproduce single operating points of the distributed DERs, a black-box model is used, which is able to capture more complex nonlinearities such as multiple operating points and device limits. Thus, the main contributions of this work are as follows:

- Propose, develop, and demonstrate an NN-based black-box model that can reproduce the aggregated behaviour of distributed BESSs providing different services, i.e., frequency regulation, oscillation damping, constant power injections, and voltage regulation.
- Propose a methodology to optimize the topology of a black-box model based on Genetic Algorithms (GAs), which also reduces the NN's training times and the black-bos model's sensitivity to small variations or noise in its inputs, while improving the robustness of the model.
- Illustrate the impact of distributed BESSs on a benchmark transmission system, for different grid contingencies, based on a benchmark ADN.

The rest of the paper is organized as follows: In Section II, an overview of BESS models and controls is presented, and the simulation-based methodology for aggregation of DERs is discussed. In Section III, the methodology to obtain an NN-based aggregated black-box model is proposed. In Section IV, the methodology is applied using measurements obtained from detailed simulations of transmission and distribution benchmark test systems, and the aggregated BESS validated. Finally, the main conclusions of the present work and scope of future work are presented in Section V.

II. Background Review

A. BESS Models and Controls

A typical BESS comprises battery cells connected in banks, which are charged and discharged through bidirectional buck-boost converters, connected to the ac grid through Voltage Source Converters (VSCs) and filters to reduce harmonics, as illustrated in Fig. 1.

In the models in [16] and [17], the internal control logic allows the BESS to provide services such as frequency regulation, voltage regulation, OD, or to operate in constant active power or constant power factor, depending on control flags that are manually defined. Once the flags are set up, the BESS operates automatically based on its control input signals, namely voltage, frequency, and/or powers. The control input setpoints can be defined at the local bus where the BESS is connected (distributed control), or can be provided

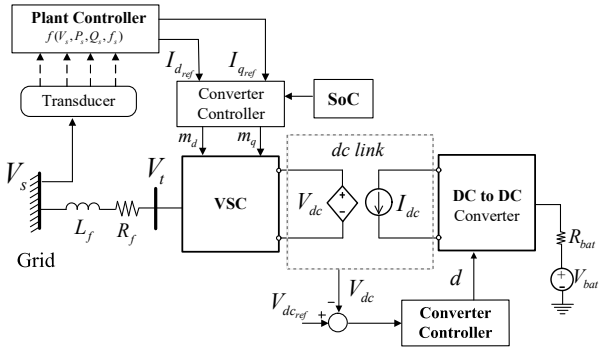


Fig. 1. Block diagram of a BESS [16].

by an entity aiming to coordinate the operation of multiple distributed BESSs (centralized control). The input setpoints and signals define the VSC dq reference current values $I_{d_{ref}}$ and $I_{q_{ref}}$, which are used in the converter current controller to determine its modulation ratios m_d and m_q, and eventually the active and reactive powers injected by the BESS. In addition to the control systems, the BESS model considers the dynamics of the ac filter R_f and L_f connecting the VSC to the power grid, the dc-to-dc converter feeding dc power to the VSC, and the dc-to-dc converter control, whose main purpose is to maintain the dc link voltage V_{dc} constant through the duty cycle d control.

B. Black-box Models

In simulation-based system aggregation, simulation data is used to determine an aggregated NN system model, whose parameters are adjusted until the NN outputs match the available measurements, using an iterative process based on the estimation errors as the main criteria for model weight adjustments (e.g. [18]).

Black-box models based on NN are widely utilized to represent highly non-linear complex systems, as in the case of simulation-based aggregated models. These NN models map inputs and outputs, based on a connectionist structure that aims to resemble the structure of a human brain, i.e., multiple nodes (neurons) interconnected with each other and exchanging information [19]. The basic processing unit in an NN is the neuron, which is characterized by a set of input connections, an activation function, and a set of outputs. NNs are structured in layers, with the input and output layers handling the input and output signals of the network, and neurons distributed among the layers. The most common structure is the feedforward NN, in which the neurons' outputs from one layer are feed as inputs of the next layer, so that the information flows in one direction. Every input is characterized by a weight that represent the state of the NN, with its main feature being its learning capability, which is accomplished by weight adjustments.

Nonlinear Autoregressive Exogenous (NARX) NNs are particularly effective to model dynamic systems [18], [20]. NARX NNs are a subclass of recurrent NNs, which perform better than conventional recurrent NNs in terms of learning capability, speed of convergence, and accuracy [20]. Hence, since

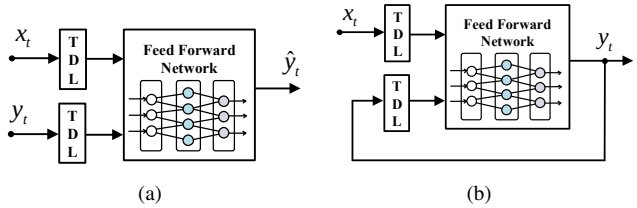


Fig. 2. NARX NN in (a) open-loop and (b) closed-loop configurations.

many NNs are trained and tested as part of the algorithm to develop black-box models in this paper, speed of convergence plays a major role, and thus NARX NNs are used here for the proposed black-box models. The NARX NN estimates the output of the system $\hat{y}_t$ to be replicated at time t as a function of past measurements of the system's output, given by, $y_{t-1}, y_{t-2}, .., y_{t-n_y}$ and the current and past measurements of the inputs $x_t, x_{t-1}, .., x_{t-n_x}$, as follows [18]:

$$\hat{y}_t = G\begin{pmatrix} y_{t-1}, y_{t-2}, ..., y_{t-n_y}, \\ x_t, x_{t-1}, x_{t-2}, ..., x_{t-n_x} \end{pmatrix} \quad (1)$$

This configuration is referred to as an open-loop configuration. Alternatively, the estimated NARX NN's output can be calculated as a function of past estimated outputs $\hat{y}_{t-1}, \hat{y}_{t-2}, , .., \hat{y}_{t-n_y}$, and current and past inputs $x_t, x_{t-1}, .., x_{t-n_x}$, which is referred to as a closed-loop configuration, as follows:

$$\hat{y}_t = G\begin{pmatrix} \hat{y}_{t-1}, \hat{y}_{t-2}, ..., \hat{y}_{t-n_y}, \\ x_t, x_{t-1}, x_{t-2}, ..., x_{t-n_x} \end{pmatrix} \quad (2)$$

where G is the NN mapping function, and n_x and n_y are the number of input and output past information or delays, respectively. Fig. 2 illustrates the open- and closed-loop configurations, where the TLD blocks represent time delays applied to their inputs; note that the main difference between open-loop and closed-loop configurations is that the latter does not need information of the actual system output, as the NN's output values $\hat{y}_{t-1}, \hat{y}_{t-2}, .., \hat{y}_{t-n_y}$ are fed back to the network. The NARX-NN's G function can be implemented as a feedforward NN with the corresponding input and output delays feeding the first hidden layer [21].

III. Aggregated BESS Model

In this section, a methodology to obtain an aggregated black-box BESS model at the boundary bus between the transmission and distribution systems is proposed. The model is based on NNs representing active and reactive power injections, whose topologies are optimized using GAs, with parameters (weights) obtained by training the NNs based on data from measurements of active and reactive power, voltage, and frequency at the boundary bus. It is assumed that the BESSs are connected to an ADN and includes PV generation, since this type of generation is becoming the dominant supply source in ADNs, instead of diesel generators or wind turbines. Significant penetration of PV generation is being deployed in various jurisdictions, with BESS being considered to enhance and facilitate their integration [22], [23].

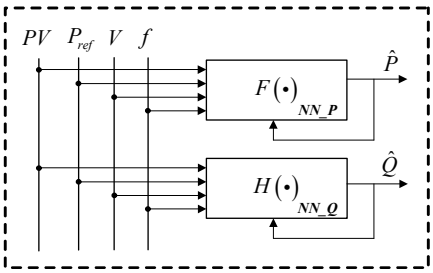


Fig. 3. Proposed aggregated black-box model for distributed BESS.

Nevertheless, aggregated models of other types of generation could be readily considered in the proposed black-box model without loss of generality.

It is important to mention that a black-box model based on a single NN to predict the P and Q outputs of aggregated BESSs yields poor results, particularly for P. The reason being, for the same events (e.g., contingency), the outputs of P and Q are different from each other, given the decoupled P and Q controls of the BESS; therefore, in the NN training process, the weights are adjusted to reduce the error of one of the outputs more than the other, resulting in an NN structure that performs better when predicting one of the outputs as opposed to both simultaneously. Hence, two NNs are proposed here, namely, NN-P and NN-Q, as black-box models to predict the P and Q outputs, respectively, of the aggregated BESSs.

A. Proposed Black-box Model

The proposed black-box model is presented in Fig. 3, which consist of two NARX NN in closed-loop configuration, NN-P and NN-Q, whose outputs represent the active (P) and reactive (Q) power injections of the aggregated BESSs at the boundary bus, and are calculated as follows:

$$\hat{P}_t = F\begin{pmatrix} \hat{P}_{t-1}, \hat{P}_{t-2}..., \hat{P}_{t-n_y}, \\ f_t, f_{t-1}, ..., f_{t-n_x}, \\ V_t, V_{t-1}, ..., V_{t-n_x}, \\ \Delta P_{ref_t}, \Delta P_{ref_{t-1}}, ..., \Delta P_{ref_{t-n_x}}, \\ PV_t, PV_{t-1}, ..., PV_{t-n_x} \end{pmatrix} \tag{3}$$

$$\hat{Q}_t = H\begin{pmatrix} \hat{Q}_{t-1}, \hat{Q}_{t-2}, ..., \hat{Q}_{t-n_y}, \\ f_t, f_{t-1}, ..., f_{t-n_x}, \\ V_t, V_{t-1}, ..., V_{t-n_x}, \\ \Delta P_{ref_t}, \Delta P_{ref_{t-1}}, ..., \Delta P_{ref_{t-n_x}}, \\ PV_t, PV_{t-1}, ..., PV_{t-n_x} \end{pmatrix} \tag{4}$$

where $\hat{P}$ and $\hat{Q}$ are estimations of the active and reactive power injections of the aggregated BESS in p.u., respectively, and assumed to be functions of the relevant measurements available at the boundary bus; V and f are the voltage and frequency at the boundary bus in p.u., respectively; ΔP_{ref} is the command signal sent from the central entity to modify the power set point of BESSs in p.u.; PV is a signal proportional to the solar irradiation, expressed as the per unit power of all PV generators; $F : \mathbb{R}^{1\times(n_y+4(1+n_x))} \rightarrow \mathbb{R}$ and $H : \mathbb{R}^{1\times(n_y+4(1+n_x))} \rightarrow \mathbb{R}$ are nonlinear functions mapping the input data, including the feedback of historical data of the estimated outputs, to the estimated outputs; and t represents the time, with a Δt time resolution, of the input data. Notice that F and H represent the internal model of the NNs proposed for the aggregation of P and Q, respectively, and depend on the structure of these networks, i.e., number of layers, number of neurons per layer, weights connecting neurons between layers, the activation function of the neurons, etc. Note that, from the description of the BESSs in Section II-A, f, V, and P_{ref} are input signals to their control systems, and therefore, should be input signals to the proposed black-box models as well, with V and f also carrying enough information of the system state. On the other hand, the PV signal provides information of the power injections of the distributed PV generation, which affect the system and BESSs operation, and is independent of the aforementioned signals, and thus needs to be taken into consideration as an additional input.

Observe in (3) and (4) that n_x and n_y denotes measurements of past input and output data (delays), respectively, which should provide a large-enough window of past information to capture the main dynamics of the BESSs response. The number of neurons in the input layer depends on the number of input signals considered in the model, which are 4 neurons for f, V, ΔP_{ref}, and PV, and 1 neuron for the output P or Q at the output layer. The number of hidden layers is often challenging to determine; intuitively, larger number of hidden layers would more accurate represent complex systems, but it is not guaranteed, and would also considerably increase the computation burden required to train the NNs. This number is considered fixed in this paper, and was determined through trial and error, based on the available measurements.

B. Aggregated Load and PV Models

Aggregated loads and PV generation can be obtained as follows [4]:

$$P_{eq_L} = \sum_j P_{L_{o_j}} V_j^{\alpha},\ Q_{eq_L} = \sum_j Q_{L_{o_j}} V_j^{\beta} \tag{5}$$

$$P_{eq_{PV}} = \sum_j P_{PV_{o_j}},\ Q_{eq_{PV}} = \sum_j Q_{PV_{o_j}} \tag{6}$$

where P_{L_o} and Q_{L_o}, and P_{PV_o} and Q_{PV_o}, are the aggregated active and reactive loads respectively, and aggregated active and reactive PV power injections of the PV generation, at each bus j of the distribution system. Note that this aggregation assumes that the PV generators are represented as constant negative power loads, as usual, and the loads behave as voltage dependent loads, with α and β exponents for P and Q respectively, as is typically the case in dynamic studies [4], especially since these represent loads on distribution feeders.

Since measurements of the active and reactive power injections at the boundary bus, represent the aggregated effect of the entire distribution system, the power injections coming from the BESS can be calculated extracting the aggregated load (5) and PV generation (6), as follows:

$$P_{BESS} = P_{Bus} - P_{eq_{PV}} + P_{eq_L} \tag{7}$$

$$Q_{BESS} = Q_{Bus} - Q_{eq_{PV}} + Q_{eq_L} \tag{8}$$

where P_{Bus} and Q_{Bus} are the measurements of active and reactive power injections at the boundary bus, respectively. Note that the aggregated BESS measurements P_{BESS} and Q_{BESS} are independent of the type of load, since the loads are extracted from P_{Bus} and Q_{Bus} measurements.

C. Training and Testing

The training of the two proposed NNs is performed based on actual measured or simulated data, for L different time series obtained from L different events. In order to use this data for training, some pre-processing is necessary, for which the algorithm depicted in Fig. 4 is used, as described next.

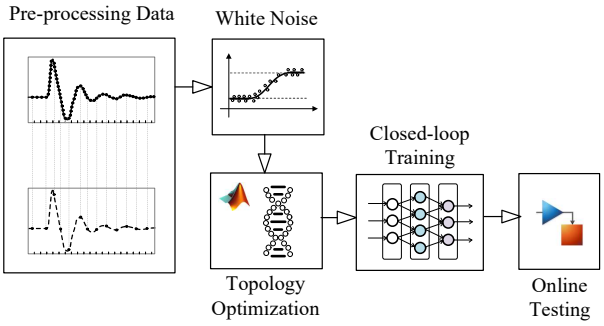


Fig. 4. Algorithm used for NN data pre-processing and NN training.

1) Data Resolution: One of the benefits of using aggregated models is the reduction of the time step of the simulations, since detailed system responses, such as those associated with BESS' converter switches, are aggregated and thus simplified. Using data with high resolution increases the training time of NNs, which is critical if several NN topologies are to be tested, when, for example, an optimal configuration is needed. Hence, the first step in the proposed algorithm is to reduce the resolution of the training data, such that the main dynamics of the system are still captured. In BESSs, the relevant time constants are in the order of ms, therefore, the data resolution should be in that range.

2) Aggregated BESS Measurements: Once the lower-resolution data is obtained, the aggregated power measurements of the BESSs P and Q are calculated using (7) and (8) for each time series l= 1,...,L.

3) White Noise Addition: White noise injection to the input data is performed before training, which is a regularization technique used to reduce overfitting and improve the robustness of the NNs, for better generalization and faster learning [24]. This helps prevent the NNs from becoming too sensitive to small disturbances, or noise introduced due to model inaccuracies, when used in simulations. The level of white noise creates a trade-off between accuracy and sensitivity, the latter observable during simulations only. Furthermore, since the output of the NNs are more sensitive to certain input signals, the level of white noise should be different for different inputs, and defined based on simulation results. Thus, white noise is added to the training data as follows:

$$x_{l,t} = \bar{x}_{l,t} + \mu_{l,t}\rho_x \max\left(\bar{\boldsymbol{x}}_l\right) \tag{9}$$

$$y_{l,t} = \bar{y}_{l,t} + \mu_{l,t}\rho_y \max\left(\bar{\boldsymbol{y}}_l\right) \tag{10}$$

where $\bar{x}_{l,t}$ is the reduced-resolution value of the input variable $x := \{f, V\}$ at time t, of the time series l; $\mu_{l,t} \sim U[0,1]$ is a random variable modeled as a uniformly distributed random process; $\bar{\boldsymbol{x}}_l$ is a vector containing all $\bar{x}_t$ of the times series l; and ρ_x is a parameter that defines the level of white noise added to the variable x with respect to its highest value in the series l. The same definitions apply for the output variables y.

4) Optimal NN Topology: The objective here is to find the vector $\boldsymbol{N}^* := [N_1^*, N_2^*, .., N_X^*]$ that contains the optimal number of neurons N_i^* per hidden layer i of the black-box NN model, which minimizes the Mean Squared Error (MSE) of the NN prediction with respect to the actual measurements used as validation data, for all time series, assuming that the total number of hidden layers X is a fixed parameter in the model. Thus, considering the highly non-linear relation between performance and topology in a NN, a GA, which is a search-based optimization technique, is used to determine $\boldsymbol{N}^*$ as follows:

$$\begin{aligned}
\min_{\boldsymbol{N}} \quad & \text{MSE} = \frac{1}{L \times M} \sum_{l=1}^{L} \sum_{k} \xi_{l,k}^2 \\
\text{s.t.} \quad & y_{l,k} - \hat{y}_{l,k} - \xi_{l,k} = 0, \quad \forall\, k \\
& G\left(\begin{array}{c} \hat{y}_{l,r-1}, \hat{y}_{l,r-2}, ..., \hat{y}_{l,r-n_y}, \\ f_{l,r}, f_{l,r-1}, ..., f_{l,r-n_x}, \\ V_{l,r}, V_{l,r-1}, ..., V_{l,r-n_x}, \\ \Delta P_{ref_{l,r}}, \Delta P_{ref_{l,r-1}}, ..., \Delta P_{ref_{l,r-n_x}}, \\ PV_{l,r}, PV_{l,r-1}, ..., PV_{l,r-n_x}, \\ \boldsymbol{w}, \boldsymbol{N} \end{array}\right) - \hat{y}_{l,k} = 0, \\
& \qquad\qquad \forall\, k = r, l = 1, ..., L \\
& \mathbf{1} \preceq \boldsymbol{N} \preceq \boldsymbol{N}_{\mathbf{max}} \\
& N_i \in \mathbb{Z}^+, \quad \forall\, i = 1, ..., X
\end{aligned} \tag{11}$$

where the vector $\boldsymbol{N} := [N_1, N_2, .., N_X]$ is part of the input variables of the NN function G, with r representing the index of all measured data points of the time series l; k is the index of the measured data points used for validation only of the time series l; M is the total number of data points k; L is the total number of time series; $\xi_{k,l}$ is the error of the predicted value $\hat{y}_{l,k}$ with respect to the measurement $y_{l,k}$, using the nonlinear function G representing the NN; $\boldsymbol{w}$ is the vector of internal weights of the NN; and $\boldsymbol{N}_{\mathbf{max}}$ is a vector that contains the maximum number of neurons per layer i. Note that the only variables in this problem are the entries of the vector $\boldsymbol{N}$.

The optimization problem described in (11) is solved using a GA, where $\boldsymbol{N}$ is a member of the population C_g, updated at every generation $g+1$, based on the individuals $\boldsymbol{N}$ that had the best performance toward minimizing the objective function, i.e., minimum MSE on the validation data set. Note that, since the NN must be trained for each candidate solution $\boldsymbol{N}$ in order to obtain the output of G, and that the objective at this stage of the algorithm is to determine the optimal topology of NN, early stopping of the training process is enforced, which reduces the time required by the GA to solve the problem. The output of this stage is the optimal topology $\boldsymbol{N}^*$.

5) Black-box Model Training: Finally, using $\boldsymbol{N}^*$, the NN is trained considering a larger number of maximum epochs

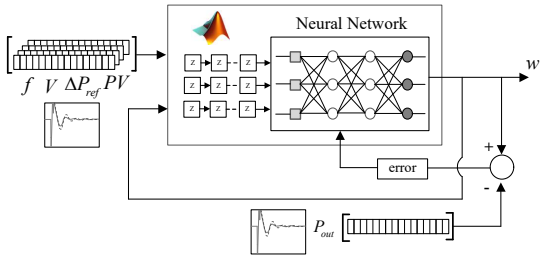


Fig. 5. NNs training process.

to obtain the lowest possible error, and thus determine the optimal vector of weights $\boldsymbol{w}$, as shown in Fig. 5.

IV. Results

The aggregated BESS model is validated through simulations using the methodology proposed in Section III, to obtain a black-box model of aggregated BESSs distributed within a modified version of the American CIGRE Medium-Voltage (MV) test ADN in [25], connected at Bus 5 of an also modified WSCC 9-bus benchmark transmission system [26], [27], which are both simulated in TSAT [28]. The aggregated BESS model is validated through simulations. Thus, the results discussed hereafter demonstrate the effectiveness of the proposed model to reproduce the behaviour of the detailed model, without loss of generality, it should apply to any interconnected transmission and distribution grids, given the general and well-accepted dynamic models used in the presented simulations.

A. Test System

In order to reduce the simulation complexity, all loads and low-voltage networks are considered balanced and aggregated at the MV/LV transformers. All breakers in the system are closed, resulting in feeder loops. A high penetration of PV generation is assumed, with storage capacity spread across the distribution system, i.e., small units at households and larger units all aggregated at the MV level, corresponding to an equivalent 1.5 MVA PV and 1.5 MVA BESS at each of the 14 buses of the ADN, as depicted in Fig. 6. The BESS are modeled based on [16], and since the scope of this paper is on BESS aggregation, simplified models for the loads and PV generation are used, as discussed in Section III; the loads are modeled as constant impedance loads, assuming α=β=2, and the PVs as negative constant power loads. The Bus 0 of the ADN is connected to Bus 5 of the WSCC 9-bus benchmark system, through a 115kV/230kV step-up transformer, representing a sub-transmission system, with parameters extracted from [25]. Single-phase detailed representations of the BESS were implemented in Powertech's power system software package TSAT [28], based on [16], requiring a time step of 0.101ms to ensure convergence, since the program did not converge with a 0.1ms time step.

The transmission system comprises one hydro generator Gen1, and two steam generators Gen 2 and Gen 3, which supply three loads, while also providing Primary Frequency Regulation (PFR) and voltage control. The steady-state data of the WSCC 9-bus test system was extracted from [26], and its dynamic data from [27], including the machines' excitation systems and Power System Stabilizers (PSS).

B. Simulated Cases

The detailed BESS model discussed in Section III is used to simulate seven cases, in which contingencies are applied in the transmission system, while the BESSs are set to operate in different modes, i.e., PFR, Oscillation Damping (OD), and constant active power (PC), as per [16]. Measurements of the active and reactive power injections, voltage, and frequency at Bus 0 of the ADN are recorded to obtain the aggregated BESS model. In all cases, the BESSs are set to initially operate in discharging mode, supplying 0.1 MW each, and the PVs injecting 0.75 MW, without loss of generality. Hence, in normal operating conditions, the ADN is consuming power from the transmission system. Also, to provide reactive power compensation, the BESSs provide voltage regulation at their local buses in all cases, to maintain the distribution system bus voltages within acceptable limits in the MV test system (between +6%/- 6%) [29]. Furthermore, step changes in the PV power are also simulated in all cases, to represent variations in the solar irradiance, as follows: {8s, +0.1p.u.}, {12s, +0.1p.u.}, and {14s, -0.1p.u.}.

The seven study cases are the following:

- Case 1: The power of Gen 2 is reduced by 10% at t=3 s, to simulate sudden generation loss; all BESSs are set to operate in PFR mode using local frequency measurements (distributed control); and the PSS of the three generators are active.
- Case 2: Same as Case 1, but the power of Gen 3 is reduced by 20% at t=3 s.
- Case 3: Same as Case 1 and 2, but the power of Gen 1 is reduced by 30% at t=3 s.
- Case 4: A Short Circuit (SC) is applied at Bus 8 at t=3 s, and then removed after 50 ms, while all BESSs are operating in OD mode, and the PSS of the three generators are disabled. In this case, the BESSs receive the same frequency signal (f at Bus 0) for the OD control, assuming that a single entity at the distribution system level controls the BESSs (centralized control).
- Case 5: Same as Case 4, but the SC is applied at Bus 6.
- Case 6: No contingency is simulated on the transmission system, but the reference power of the 14 BESSs is changed by +0.5 p.u. at t=3 s, when operating in PQ mode and in centralized control mode, to simulate a sudden increase in the power supplied by the ADN.
- Case 7: Same as Case 6, but all BESS powers are changed by -0.5 p.u. at t=3 s, to simulate a sudden decrease in the power supplied by the ADN.

These cases are summarized in Table I. The duration of the simulations for all cases is 22s. Note that at least two time series per type of service and contingency are simulated, which activate most the BESSs' controller branches (except the contact power factor control) and excite the relevant system dynamics, which provide quality data to train the black-box model to accurately represent the aggregated BESSs for these

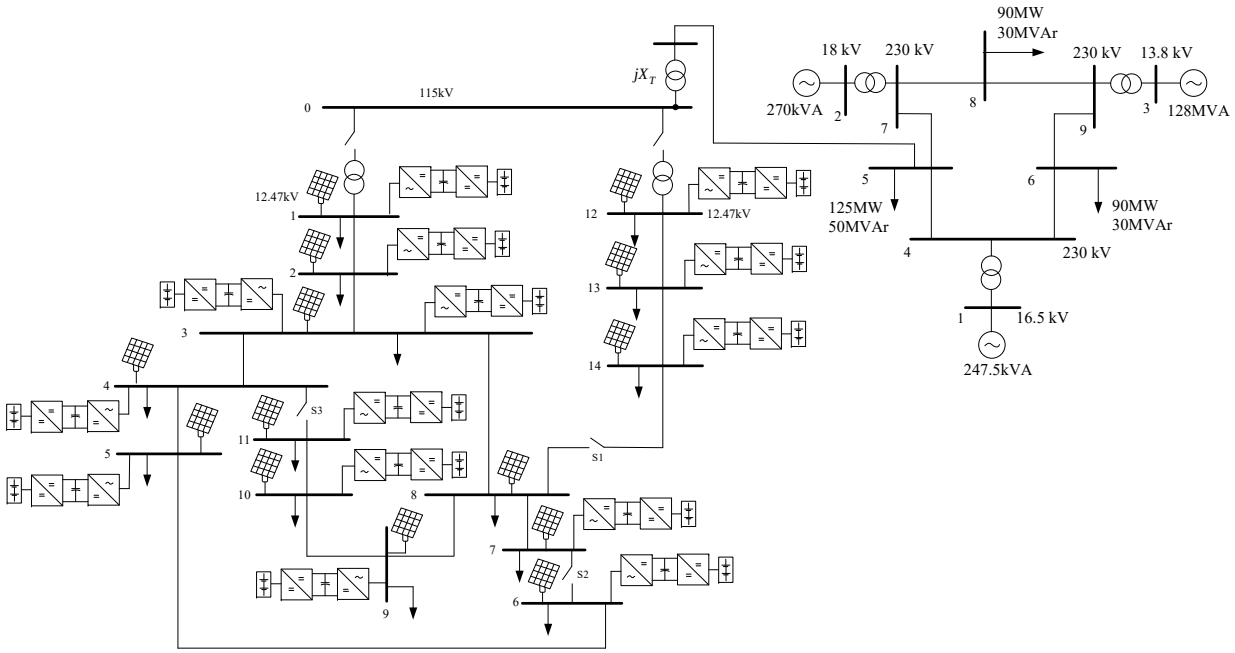


Fig. 6. Transmission-ADN test system.

contingencies, as well as untrained events, as demonstrated next.

TABLE I
SIMULATED CASES

Case	Contingency	BESS Control			PSS
		P	Q	Input Δf	
1	+10%ΔP Gen 2	PFR	V Reg.	Local	Yes
2	+20%ΔP Gen 3	PFR	V Reg.	Local	Yes
3	+30%ΔP Gen 1	PFR	V Reg.	Local	Yes
4	SC Bus 8	OD	V Reg.	Central	No
5	SC Bus 6	OD	V Reg.	Central	No
6	+0.5ΔP_{BESS}	PC	V Reg.	Central	Yes
7	-0.5ΔP_{BESS}	PC	V Reg.	Central	Yes

The main assumptions considered in developing the aggregated BESS model are the following:

- All BESSs independently operate in the same control mode in each case, i.e., PFR, OD, and PC, described in [16]. Different control modes are used depending on the contingency simulated.
- All BESSs regulate the local voltage in all cases.
- The input signals to the black-box BESS model are the bus frequency and voltage at the boundary bus between transmission and distribution systems, a signal (PV) proportional to the solar irradiance, and a signal (ΔP_{ref}) proportional to the change in the BESSs' power reference.
- All PVs added to the ADN have the same power ratings and produce the same active power, but in principle, these could have different ratings and P outputs, without impacting the proposed modeling approach.
- The nominal load and ADN topology are the same as in the original CIGRE MV test system, in all cases.
- All BESSs have the same ΔP_{ref} in Cases 6 and 7.
- The events simulated excite the relevant internal BESSs' dynamics.
- The topology of the ADN does not change, and seasonality of data is not considered.

C. BESS Black-box Model Parameters

The methodology proposed in Section III-C is applied here to obtain the aggregated black-box BESS model, for which simulated measurements at Bus 0 of the ADN are used to train the two NNs, NN-P and NN-Q. The TSAT simulations had a data resolution of 0.101 ms, which represents around 220,000 data points per input per case; hence, training the NNs with that resolution requires 7.7 million data points for the seven cases considered, for all the inputs and output feedback, per NN. This presents a computational challenge, because of the large number of operations required while adjusting the NNs' weights during training. Hence, the data resolution was reduced to 0.01 s, as explained in Section III-C1, which considerably reduced the computational burden, while capturing the main dynamics of the aggregated behaviour of the BESSs, relevant for typical transient stability studies. Furthermore, five measurements of past data of the inputs and outputs are used in (3) and (4), since it provides a large-enough window of historic information observed by the model, as demonstrated in the next section. The aggregation of the BESSs was performed using (7) and (8).

To determine the level of white noise required to obtain adequate black-box models, a sensitivity analysis of the inputs to the NNs was performed, starting with finding the optimal NN configuration without considering white noise. Then, the NN with the optimal configuration was trained, adding white noise to the input data and observing how the MSE values change for the trained and untrained events, noticing that as the

level of white noise increased, the MSE slightly increased for the trained events, but considerably decreased for the untrained events. Hence, the white noise levels were increased until acceptable MSE values were obtained for both the trained and untrained events. These white noise levels were then applied to the input data to obtain a new optimal NN configuration. This trial-and-error approach yielded. This empirical process yielded $\rho_x = \rho_y = 0.003$ for (9) and (10).

In [14], two hidden layers are proposed in a black-box model representing the response of an aggregated system based on microturbines, to one type of disturbance only; however, three different disturbances in the seven studied cases ($L = 7$) are considered here, with the addition of PVs changing their output power within the distribution system, which requires a more complex structure. Indeed, when less than 4 hidden layers were studied (e.g., 2 and 3), poor performance in the predictive capability of the NNs was observed, resulting in too many topologies. On the other hand, more than four layers increased considerably the domain of the problem making it intractable, since the number of possible topologies increases exponentially with the number of hidden layers. Hence, four hidden layers $X = 4$ for NN-P and NN-Q are considered, since it increases the capability of the NNs, while keeping the computational burden reasonable, and yielding adequate results as demonstrated here. Furthermore, the number of neurons per layer are constrained to 50, to reduce the population domain in the GA. The activation function used for the neurons is the sigmoid function. Each case described in Section IV-B corresponds to the time series l that is used to train the NNs, with 70% of the available data of each time series being used for training, 25% for validation, and 5% for testing.

The following optimization problems are then solved using GAs, to obtain the optimal topology of NN-P and NN-Q:

$$
\begin{aligned}
\min_{\boldsymbol{N_p}} \quad & \text{MSE} = \frac{1}{7 \times M} \sum_{l=1}^{7} \sum_{k} \xi_{p_{l,k}}^2 \\
\text{s.t.} \quad & P_{l,k} - \hat{P}_{l,k} - \xi_{l,k} = 0, \quad \forall\, k \\
& F \left(\begin{array}{c} \hat{P}_{l,r-1}, \hat{P}_{l,r-2}, ..., \hat{P}_{l,r-5}, \\ f_{l,r}, f_{l,r-1}, ..., f_{l,r-5}, \\ V_{l,r}, V_{l,r-1}, ..., V_{l,r-5}, \\ \Delta P_{ref_{l,r}}, \Delta P_{ref_{l,r-1}}, ..., \Delta P_{ref_{l,r-5}}, \\ PV_{l,r}, PV_{l,r-1}, ..., PV_{l,r-5}, \\ \boldsymbol{w_p}, \boldsymbol{N_p} \end{array} \right) - \hat{P}_{l,r} = 0, \\
& \qquad\qquad \forall\, r \wedge l = 1, ..., 7 \\
& \mathbf{1} \preceq \boldsymbol{N_p} \preceq N_{p_{\max}} \boldsymbol{I} \\
& N_{p_i} \in \mathbb{Z}^+, \quad \forall\, i = 1, ..., 4
\end{aligned}
\tag{12}
$$

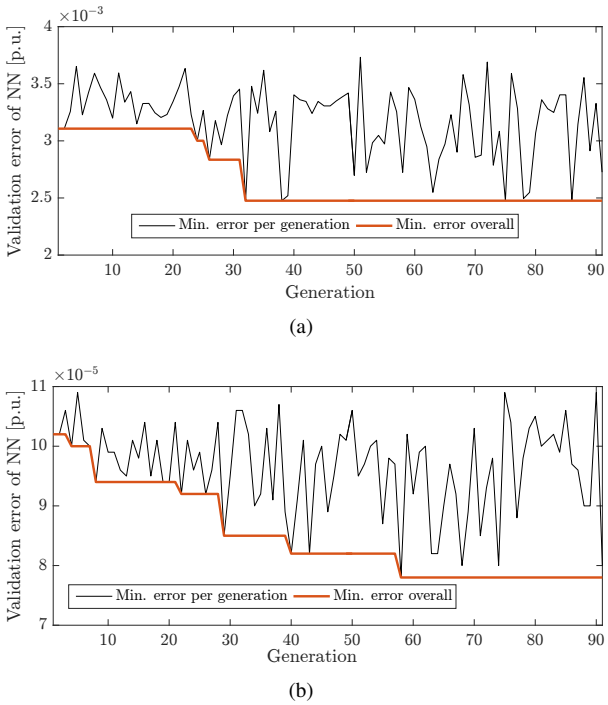


Fig. 7. Evolution of the MSE per generation of (a) NN-P and (b) NN-Q.

$$
\begin{aligned}
\min_{\boldsymbol{N_Q}} \quad & \text{MSE} = \frac{1}{7 \times M} \sum_{l=1}^{7} \sum_{k} \xi_{Q_{l,k}}^2 \\
\text{s.t.} \quad & Q_{l,k} - \hat{Q}_{l,k} - \zeta_{l,k} = 0, \quad \forall\, k \\
& H \left(\begin{array}{c} \hat{Q}_{l,r-1}, \hat{Q}_{l,r-2}, ..., \hat{Q}_{l,r-5}, \\ f_{l,r}, f_{l,r-1}, ..., f_{l,r-5}, \\ V_{l,r}, V_{l,r-1}, ..., V_{l,r-5}, \\ \Delta P_{ref_{l,r}}, \Delta P_{ref_{l,r-1}}, ..., \Delta P_{ref_{l,r-5}}, \\ PV_{l,r}, PV_{l,r-1}, ..., PV_{l,r-5}, \\ \boldsymbol{w_Q}, \boldsymbol{N_Q} \end{array} \right) - \hat{Q}_{l,r} = 0, \\
& \qquad\qquad \forall\, r \wedge l = 1, ..., u \\
& \mathbf{1} \preceq \boldsymbol{N_Q} \preceq N_{Q_{\max}} \boldsymbol{I} \\
& N_{Q_i} \in \mathbb{Z}^+, \quad \forall\, i = 1, ..., 4
\end{aligned}
\tag{13}
$$

A summary of the parameters for (12) and (13) is presented in Table II. The size of the population of the GA is 1000 individuals, and the maximum number of epochs for the training of each candidate NN is limited to 500. The convergence criteria used for the GA is a maximum 200 generations, or 50 consecutive generations without reducing the minimum MSE. The evolution of the MSE of NN-P and NN-Q, per generation, is presented in Fig. 7. More than 92,000 different candidate topologies for NN-P and NN-Q were trained and validated against their corresponding available measurements,

TABLE II
NN-BASED BLACK-BOX MODEL CONFIGURATION

Parameter	Value	Parameter	Value
n_x	5	n_y	5
$N_{p_{\max}}$	50	$N_{Q_{\max}}$	5
m	550	L	7
X	4		

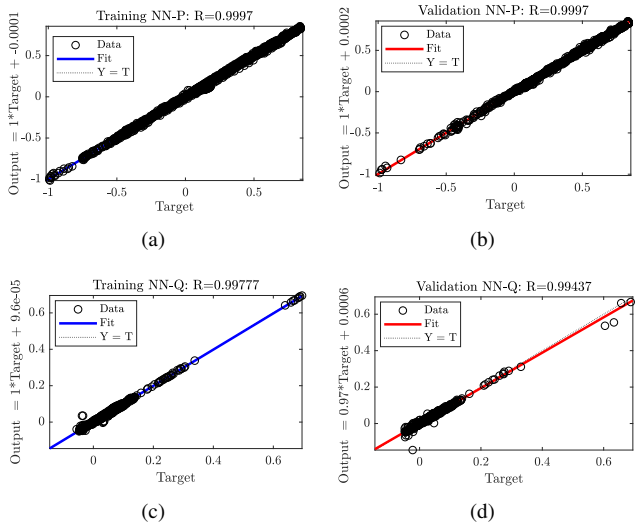


Fig. 8. Correlation coefficient R for (a) training and (b) validation data for NN-P; and (c) training and (d) validation data for NN-Q.

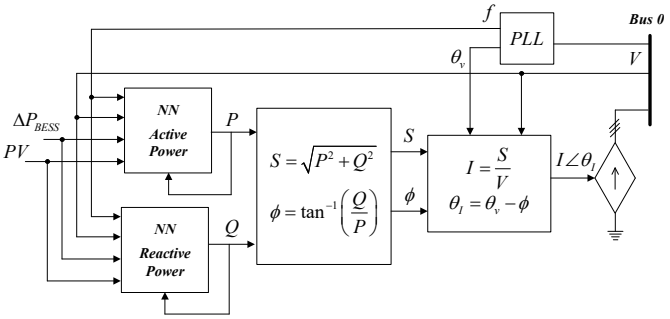


Fig. 9. Simulink interface for the aggregated BESS model.

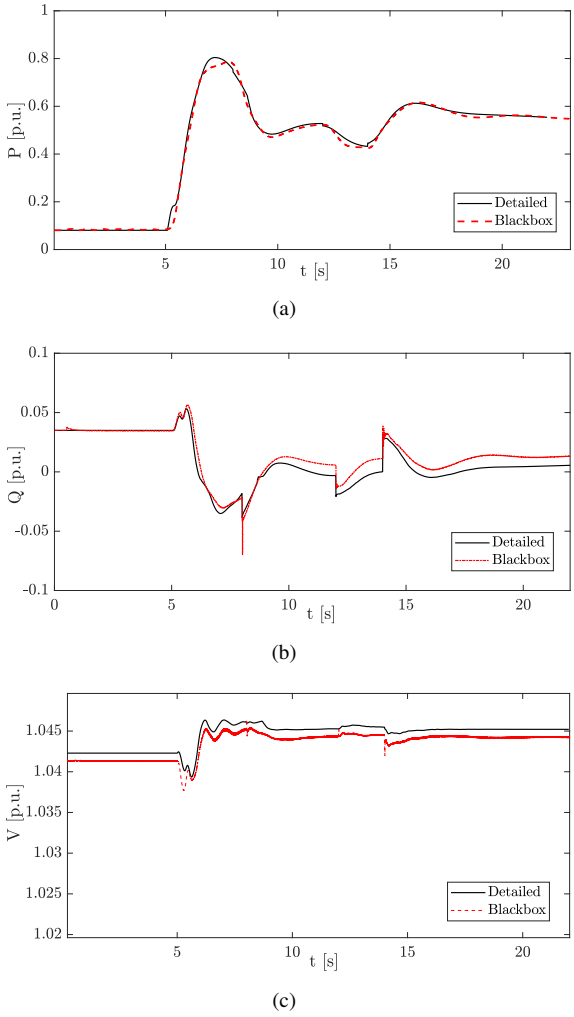


Fig. 10. Aggregated BESS output for Case 1 (a) P, (b) Q, and (c) V.

resulting in the optimal configurations: $\boldsymbol{N_P}^* = [40, 16, 37, 5]$ and $\boldsymbol{N_Q}^* = [23, 49, 33, 19]$.

Based on $\mathbf{N_P}^*$ and $\mathbf{N_Q}^*$, the NN-P and NN-Q are then obtained by increasing the maximum number of epochs for training to 1000. The performance regression of prediction using NN-P and NN-Q for the training and validation data is presented in Fig. 8. Note that a good prediction was obtained, yielding correlation coefficients close to 1. The MSE of the validation data considering the seven time series for NN-P and NN-Q were 7.499×10^{-5} p.u. and 1.282×10^{-5} p.u., respectively.

D. Model Validation in Simulink

In order to validate the proposed aggregated BESS black-box model in simulations, the transmission system discussed in Section IV-A with the proposed NN-P and NN-Q aggregated BESS models were implemented in Matlab's Simulink. The black-box model is effectively integrated in the simulations as a controllable current source connected at Bus 0, which requires the interface presented in Fig. 9. Note that $\hat{P}$ and $\hat{Q}$ are used to calculate the current I injected at Bus 0, by dividing the aggregated BESS apparent power S by the measured terminal voltage V, while the current angle θ_I is obtained by subtracting the power factor angle ϕ from the voltage phase angle θ_V. The frequency measurements f and θ_V are obtained through a PLL circuit.

A comparison between the detailed model and simulations based on the proposed aggregated black-box BESS models was performed for all the cases described in Section IV-B. In Figs. 10, 11, and 12 the simulation results for Cases 1, 4, and 6, are presented, respectively, since these are the most relevant. In Cases 1 (Figs. 10a, 10b, and 10c), 2, and 3, the BESSs, operating in local control mode, provides PFR, thus increasing their active power injections to help stabilize the dropping frequency resulting from the power reduction of the generators in the transmission system. Notice that the system frequency is also affected by the changes in the PV generation within the distribution system, which occurs at 8 s, 12 s, and 14 s; furthermore, since the PV input signal to the NN-P and NN-Q also changes at these times, fast transients that quickly disappear are observed in P and Q. Observe that the NN-P can accurately reproduce the aggregated active power injections P. On the other hand, the NN-Q outputs follow very closely the reactive power curves obtained with the detailed model with a small offset, which is due to the fact that the initial steady-state voltage at Bus 0 in the Simulink simulations is slightly larger

than that in the original TSAT detailed model, as observed in Fig. 10c. Furthermore, the variations in the PVs generation has a direct impact on the voltage regulation capability of the BESS, as the PV sources are physically located at the same buses as the BESSs.

The results of Cases 4 (Figs. 11a, 11b, and 11c) and 5, demonstrate, first, that proper control of distributed BESSs can help to damp low-frequency oscillations at the transmission level, and, second, that the NN-P and NN-Q are able to properly represent the aggregated BESS response, even though the system response is considerable different from those obtained in the previous cases. Notice that the NN-P tends to produce P values slightly larger than those in the detailed model, thus reducing the system oscillations faster. Similar results are observed in Cases 6 (Figs. 12a, 12b, and 12c) and 7, where, while P remains constant, changing only when the NN-P receives a ΔP_{ref} command, Q varies according to the voltage regulation requirements at the local buses.

Based on the aforementioned results, the proposed black-box model is shown to be robust enough with respect to grid component model inaccuracies, as the measurements were obtained in TSAT [28], while the black-box model simulations were performed on Matlab's Simscape based on three-phase models [30], with somewhat different component models. Furthermore, the interface depicted in Fig. 9 was introduced to connect the black-box model to the transmission grid. This interface introduced differences between the models and simulations, and their actual application and validation.

In order to demonstrate the generalization capability of the proposed model, two additional cases, for which the NNs were not trained, were simulated. Thus, in Figs. 13a, 13b, and 13c, the response of the aggregated BESSs providing PFR for a reduction of 5% in the power of Gen 2 (Case 8) is presented; and in Figs. 14a, 14b, and 14c, their aggregated response while providing oscillation damping for a 50 ms short circuit at Bus 9 of the transmission system (Case 9) is depicted. Observe that the main trend of P and Q are still adequately reproduced in both cases, with a more significant difference for P and Q in Case 8.

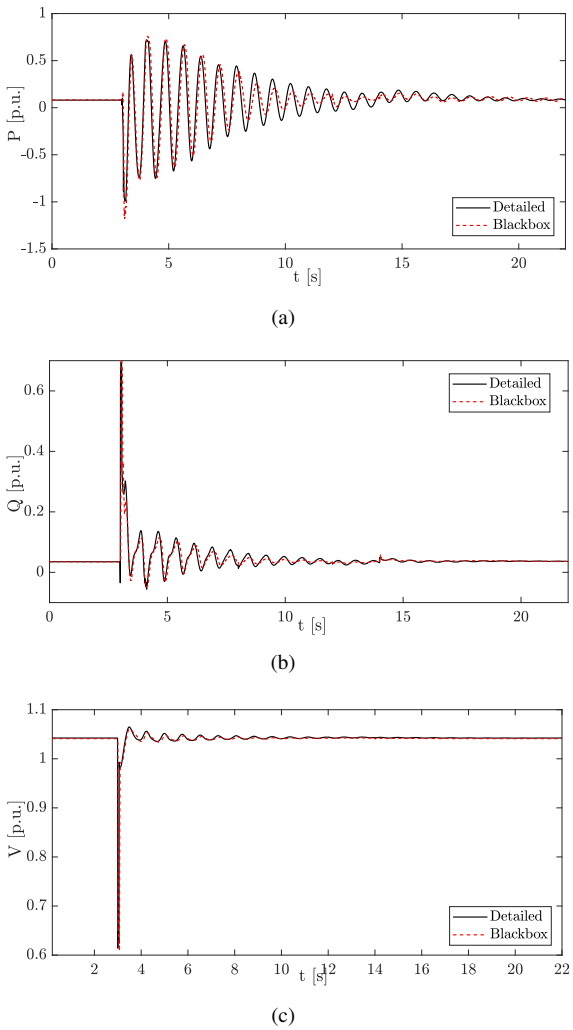


Fig. 11. Aggregated BESS output for Case 4 (a) P and (b) Q, and (c) V.

V. Conclusions

In this paper, black-box models proposed to represent the aggregated response of BESSs connected at the distribution level for contingencies at the transmission level. The models comprised two NNs, one for P and the other for Q, whose topology was obtained using a GA-based algorithm to determined the optimal number of neurons in the hidden layers. The NNs were trained, validated, and tested with data for nine different transmission system contingencies, demonstrating through simulations that the proposed models could accurately reproduce the results obtained from detailed models with the BESSs providing different services, while considering PV solar generation and loads. The obtained black-box models were shown to be robust, as they were able to handle white noise in their inputs without compromising the accuracy of their outputs, and were also able to represent events for which they were not trained. The model proposed in this paper can thus be readily applied by transmission system operators for studies where PV systems with storage capacity are massively deployed, or as a planning tool to estimate the effects of increasing penetration of distributed PV generation and BESS on distribution systems.

References

[1] J. H. Chow, R. Galarza, P. Accari, and W. W. Price, "Inertial and slow coherency aggregation algorithms for power system dynamic model reduction," *IEEE Trans. Power Syst.*, vol. 10, no. 2, pp. 680–685, 1995.

[2] T. Y. J. Lem and R. T. H. Alden, "Comparison of experimental and aggregate induction motor responses," *IEEE Trans. Power Syst.*, vol. 9, no. 4, pp. 1895–1900, 1994.

[3] P. Jazayeri, W. Rosehart, and D. T. Westwick, "A multistage algorithm for identification of nonlinear aggregate power system loads," *IEEE Trans. Power Syst.*, vol. 22, no. 3, pp. 1072–1079, 2007.

[4] P. Kundur, *Power system stability and control*. NY: McGraw-hill, 1994.

[5] J. V. Milanović and S. M. Zali, "Validation of equivalent dynamic model of active distribution network cell," *IEEE Trans. Power Syst.*, vol. 28, no. 3, pp. 2101–2110, 2013.

[6] S. M. Zali and J. V. Milanović, "Generic model of active distribution network for large power system stability studies," *IEEE Trans. Power Syst.*, vol. 28, no. 3, pp. 3126–3133, 2013.

[7] N. Fulgêncio, C. Moreira, L. Carvalho, and J. P. Lopes, "Aggregated dynamic model of active distribution networks for large voltage disturbances," *Elec. Power Syst. Research*, vol. 178, p. 106006, 2020.

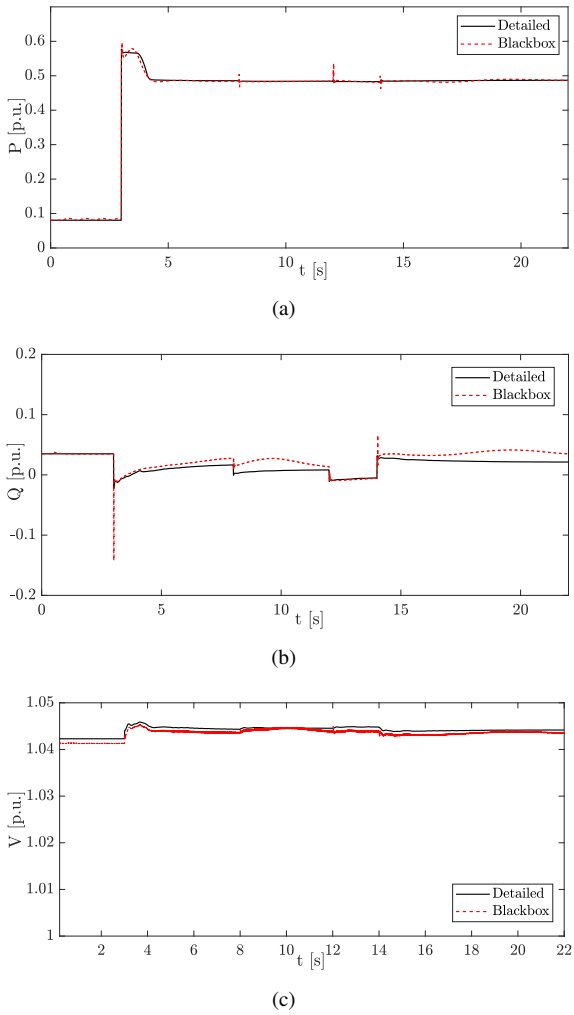


Fig. 12. Aggregated BESS output for Case 6: (a) P and (b) Q, and (c) V.

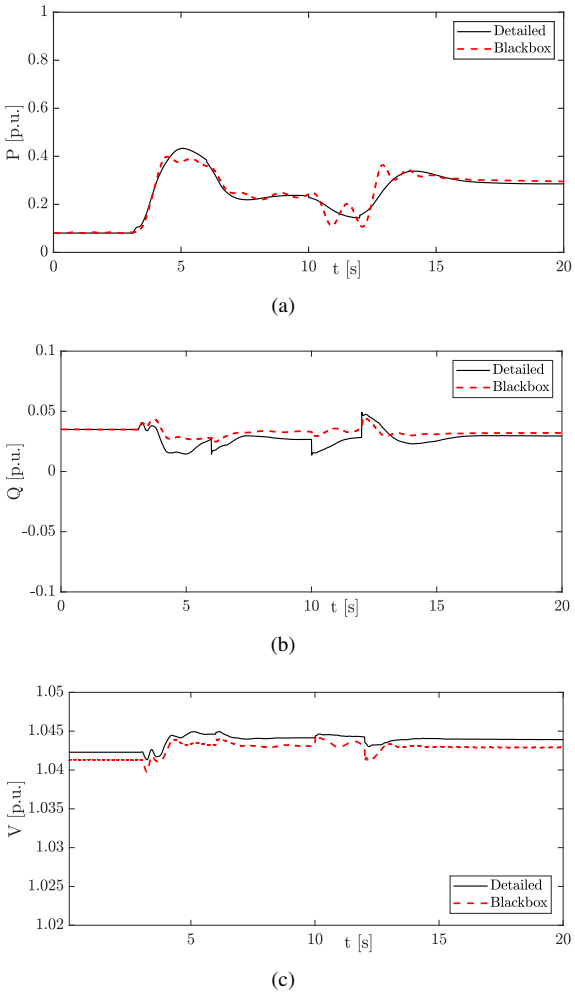


Fig. 13. Aggregated BESS output for Case 8 (a) P and (b) Q, and (c) V.

[8] ——, "Equivalent dynamic model of active distribution networks for large voltage disturbances," in *IEEE PowerTech*, Milan, Italy, June 2019, pp. 1–6.

[9] G. Chaspierre, P. Panciatici, and T. Van Cutsem, "Aggregated dynamic equivalent of a distribution system hosting inverter-based generators," in *Power Syst. Computation Conf. (PSCC)*, Dublin, Ireland, June 2018, pp. 1–7.

[10] F. Conte, F. D'Agostino, S. Massucco, G. Palombo, F. Silvestro, C. Bossi, and M. Cabiati, "Dynamic equivalent modelling of active distribution networks for TSO-DSO interactions," in *IEEE PES Innovative Smart Grid Technol. Conf. Europe (ISGT-Europe)*, Torino, Italy, Sep. 2017, pp. 1–6.

[11] X. Feng, Z. Lubosny, and J. W. Bialek, "Identification based dynamic equivalencing," in *IEEE Lausanne Power Tech*, Lausanne, Switzerland, July 2007, pp. 267–272.

[12] H. Golpîra, H. Seifi, and M. R. Haghifam, "Dynamic equivalencing of an active distribution network for large-scale power system frequency stability studies," *IET Generation, Transmission Distribution*, vol. 9, no. 15, pp. 2245–2254, 2015.

[13] M. K. Donnelly, J. E. Dagle, D. J. Trudnowski, and G. J. Rogers, "Impacts of the distributed utility on transmission system stability," *IEEE Trans. Power Syst.*, vol. 11, no. 2, pp. 741–746, 1996.

[14] A. M. Azmy and I. Erlich, "Identification of dynamic equivalents for distribution power networks using recurrent ANNs," in *IEEE PES Power Systems Conference and Exposition.*, New York, NY, Oct. 2004, pp. vol 1. 348–353.

[15] C. Han, D. Changhong, and Li Dalu, "Recurrent neural network-based dynamic equivalencing in power system," in *IEEE International Conference on Control and Automation*, Guangzhou, China, May 2007, pp. 2396–2399.

[16] F. Calero, C. A. Cañizares, and K. Bhattacharya, "Dynamic Modeling of Battery Energy Storage and Applications in Transmission Systems," *IEEE Transaction on Smart Grid*, August 2020, 10 pages.

[17] "WECC battery storage dynamic modeling guideline," Tech. report, WECC, Modeling and Validation Work Group, pp. 1–38, 2016.

[18] Z. Boussaada, O. Curea, A. Remaci, H. Camblong, and N. Mrabet Bellaaj, "A nonlinear autoregressive exogenous (NARX) neural network model for the prediction of the daily direct solar radiation," *Energies*, vol. 11, no. 3, pp. 1–21, 2018.

[19] F. Karray, F. O. Karray, and C. W. De Silva, *Soft computing and intelligent systems design: Theory, tools, and applications*. Pearson Education, 2004.

[20] M. S. H. Lipu, M. A. Hannan, A. Hussain, M. H. Saad, A. Ayob, and F. Blaabjerg, "State of charge estimation for lithium-ion battery using recurrent NARX neural network model based lighting search algorithm," *IEEE access*, vol. 6, pp. 28 150–28 161, 2018.

[21] "Design Time Series NARX Feedback Neural Networks," MathWorks, 2020. [Online]. Available: https://www.mathworks.com/help/deeplearning/ug/design-time-series-narx-feedback-neural-networks.html

[22] "California Energy Commission-Tracking progress, Energy storage," California Energy Commission, Aug. Tech. Report, 2018. [Online]. Available: https://www.energy.ca.gov/sites/default/files/2019-12/energy_storage_ada.pdf

[23] "Q3/Q4 2019: Solar industry update," National Renewable Energy Laboratory (NREL), Feb. Tech. Report, NREL/PR-6A20-76158, 2020.

[24] I. Goodfellow, Y. Bengio, and A. Courville, *Deep learning*. MIT press, 2016.

[25] Strunz et al., "Benchmark systems for network integration of renewable and distributed energy resources," Tech. report, Cigre Task Force C, Apr. 2014.

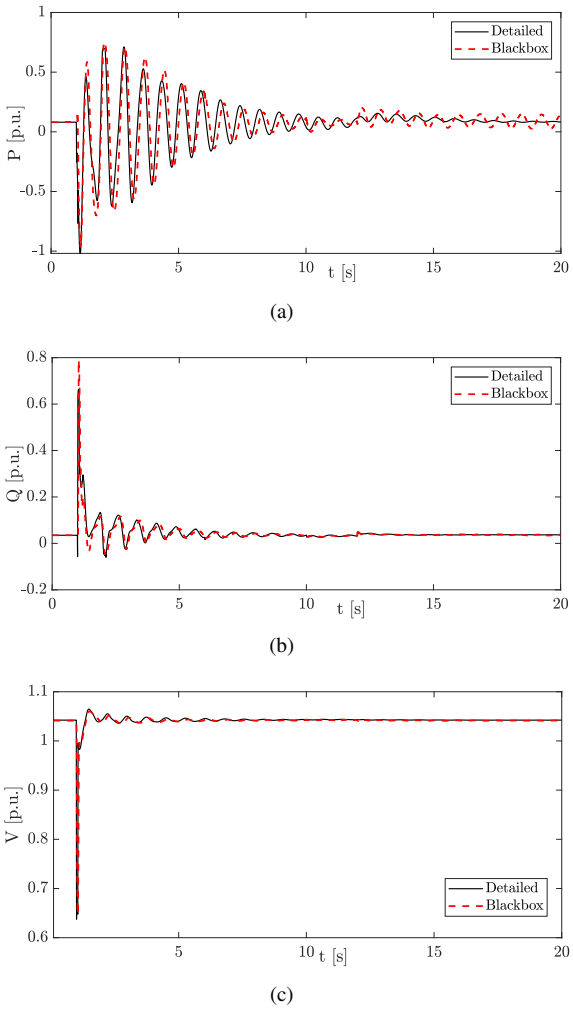


Fig. 14. Aggregated BESS output for Case 9 (a) P and (b) Q, and (c) V.

[26] P. M. Anderson and A. A. Fouad, *Power system control and stability*. NJ: John Wiley & Sons, 2008.
[27] T. Hiyama, "Rule-based stabilizer for multi-machine power system," *IEEE Trans. Power Syst.*, vol. 5, no. 2, pp. 403–411, May 1990.
[28] "TSAT transient security assessment tool model manual," Powertech Labs In., 2018. [Online]. Available: https://www.powertechlabs.com/
[29] S. McNally, "Distribution system voltage and power quality," Tech. guideline No. ECG0008, HydroOttawa, Mar. 2016.
[30] "Simscape Model and simulate multidomain physical systems," MathWorks, 2020. [Online]. Available: https://www.https://www.mathworks.com/products/simscape.html



Fabian Calero (S'18) received the diploma in electrical engineering from Escuela Politécnica Nacional (EPN), Quito, Ecuador, in 2007. He is currently pursuing the Ph.D. degree in Electrical and Computer Engineering with the University of Waterloo, ON, Canada. His research interests include power system modeling and control, and artificial intelligence applications for dynamic modelling.



Claudio A. Cañizares (S'85,M'91,SM'00,F'07) is a University Professor and Hydro One Endowed Chair at the ECE Department of the University of Waterloo, where he has been since 1993. His highly cited research focuses on modeling, simulation, computation, stability, control, and optimization of power and energy systems. He is the IEEE Trans. Smart Gird EIC; a Fellow of the IEEE, the Royal Society of Canada, and the Canadian Academy of Engineering; and is the recipient of the 2017 IEEE PES Outstanding Power Engineering Educator Award, the 2016 IEEE Canada Electric Power Medal, and of multiple awards and recognitions from PES Technical Committees..



Kankar Bhattacharya (M'95,SM'01,F'17) received the Ph.D. degree in electrical engineering from the Indian Institute of Technology, New Delhi, India, in 1993. He was with the Faculty of Indira Gandhi Institute of Development Research, Mumbai, India, from 1993 to 1998, and with the Department of Electric Power Engineering, Chalmers University of Technology, Gothenburg, Sweden, from 1998 to 2002. In 2003, he joined the Electrical and Computer Engineering Department, University of Waterloo, Waterloo, ON, Canada, where he is currently a full Professor. His current research interests include power system economics and operational aspects. He is a Registered Professional Engineer in the province of Ontario.